PROCEEDINGS OF SCIENCE

Systematic studies of beam-normal single spin asymmetries at MAMI

M. Thiel,[a,*] **A. Esser,**[a] **M. Hoek,**[a] **H. Merkel,**[a] **U. Müller,**[a] **B.S. Schlimme**[a] **and C. Sfienti**[a]

[a] *Institut für Kernphysik, Johannes Gutenberg-Universität, Johann-Joachim Becher Weg 45, D-55128 Mainz, Germany*

E-mail: thielm@uni-mainz.de, essera@uni-mainz.de, hoek@uni-mainz.de, merkel@uni-mainz.de, ulm@uni-mainz.de, schlimme@uni-mainz.de, sfienti@uni-mainz.de

Reaching new precision frontiers in nuclear physics raises new experimental challenges as well as the demand for more sophisticated theoretical calculations. Especially in parity-violation electron scattering experiments the contribution from higher order processes, such as two-photon exchange, is comparable in size with the observed asymmetry A_{PV}. Hence, a precise knowledge of this contribution is mandatory to determine the systematic uncertainties. Beam-normal single spin asymmetries A_n (or the so-called transverse asymmetries) are a direct probe of the imaginary part of the two-photon exchange amplitude in the elastic scattering of transversely polarized electrons from unpolarized nuclei. Up to now, there is significant disagreement between experiment and theory for ^{208}Pb, which motivates more measurements to study the Q^2 and Z dependence. During a successful campaign at the MAinz MIcrotron (MAMI), using the spectrometer set-up of the A1 collaboration, the Q^2 dependence of A_n for ^{12}C was determined. Follow-up experiments on ^{28}Si and ^{90}Zr investigated the charge dependence of the transverse asymmetry and have paved the way for the future experiment on ^{208}Pb, thus benchmarking the theoretical calculations in the heavier mass regime.

25th International Spin Physics Symposium (SPIN 2023)
24-29 September 2023
Durham, NC, USA

∗Speaker

PoS(SPIN2023)177

1. Introduction

Parity-violation electron scattering experiments offer excellent opportunities for investigating hadron and nuclear structure [1–6]. Due to technological progress future parity-violation experiments will constantly push the precision frontier in the exploration of the electroweak sector of the Standard Model [7–9]. For the interpretation of this high-precision data it is mandatory to go beyond the Born approximation, where the electromagnetic electron-nucleus interaction is described via the exchange of one virtual photon (OPE). Indeed, higher-order processes such as multi-boson exchanges must be taken into account. Particularly, the study of two-photon exchange (TPE) processes, as depicted in the right panel of Fig. 1, provide important input for theoretical calculations of the corresponding box diagrams in the electroweak sector. To benchmark such higher-order calculations, measurements of observables sensitive to two-photon exchange processes like the beam-normal single spin asymmetry are essential.

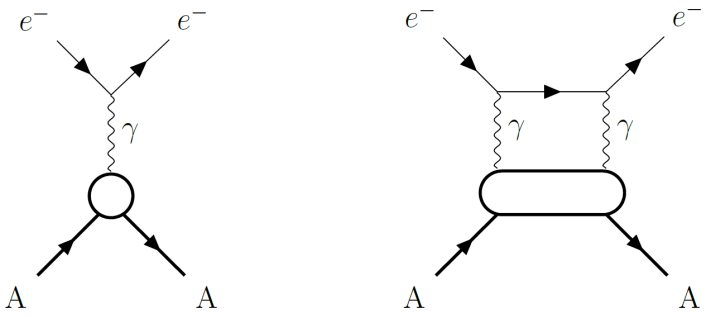

Figure 1: One-photon exchange, OPE, (*left*) and two-photon exchange, TPE, (*right*) diagrams for elastic electron-nucleus scattering.

2. Beam-normal single spin asymmetry

The beam-normal single spin asymmetry (or so-called transverse asymmetry) A_n gives direct access to the TPE process. The asymmetry arises from the interference of the one- and two (or more)-photon exchange amplitudes [10]. In the theoretical treatment of the transverse asymmetry for nuclei, the contributions of the elastic and inelastic intermediate states must be taken into account [11]. However, this calculation is limited to the very low four-momentum transfer region ($m_e c \ll Q \ll E/c$), where the transverse asymmetry is given by

$$A_n(Q^2) \propto C_0 \log\left(\frac{Q^2}{m_e^2 c^2}\right) \frac{F_{\text{Compton}}(Q^2)}{F_{\text{ch}}(Q^2)}. \tag{1}$$

The coefficient C_0 results from an energy-weighted integral over the total photoabsorption cross section. The ratio of the Compton to charge form factor $F_{\text{Compton}}(Q^2)/F_{\text{ch}}(Q^2)$ enables the calculation to be generalized to nuclear targets. Since the Q^2 dependence of the Compton scattering amplitude was only available for ^{1}H and ^{4}He, the following approximation was used in the calculation of [11]

$$F_{\text{Compton}}(Q^2) \propto e^{-BQ^2}, \tag{2}$$

where B is the Compton slope parameter. As can be seen in Eq. 1, the exact knowledge of the Compton slope parameter becomes more crucial for higher Q^2-values.

The beam-normal single spin asymmetry A_n can be accessed in electron scattering experiments and is defined as

$$A_n = \frac{\left(\frac{d\sigma}{d\Omega}\right)^{\uparrow} - \left(\frac{d\sigma}{d\Omega}\right)^{\downarrow}}{\left(\frac{d\sigma}{d\Omega}\right)^{\uparrow} + \left(\frac{d\sigma}{d\Omega}\right)^{\downarrow}}. \tag{3}$$

Here, $(d\sigma/d\Omega)^{\uparrow}$ $\left((d\sigma/d\Omega)^{\downarrow}\right)$ represents the differential cross section for electrons with spin parallel (antiparallel) to the normal vector $\hat{n}$ of the scattering plane. The experimentally measured asymmetry is related to A_n by

$$A_{\text{exp}} = A_n \vec{P}_e \cdot \hat{n}, \tag{4}$$

where $\vec{P}_e$ is the electron polarization vector.

Apart from the fact that beam-normal single spin asymmetries are essential for a better understanding of box diagrams with intermediate excited states in the electroweak sector, a detailed knowledge of this quantity is also mandatory for any parity-violation electron scattering experiment, where the electron beam has to be polarized longitudinally. Any small normal component to the beam polarization can lead to significant false asymmetries. Hence, to constrain the resulting systematic error, dedicated A_n measurements with the same kinematics and target as the parity-violation experiments are mandatory.

Previously, the PREX and HAPPEX collaborations have determined the transverse asymmetry for ^{1}H, ^{4}He, ^{12}C, and ^{208}Pb [12]. While the obtained asymmetries for the lighter nuclei were in good agreement with theoretical predictions from Ref. [11], a striking disagreement was observed for ^{208}Pb. Since the individual measurements were performed at different kinematics, a coherent picture of the beam-normal single spin asymmetry of nuclei remains elusive and requires more systematic studies in the intermediate to heavy mass regime.

3. Experimental campaign at Mainz

The measurement of the beam-normal single spin asymmetry imposes high demands on the accelerator and the experimental set-up. The MAinz MIcrotron (MAMI) is able to deliver high beam currents of excellent quality with a high degree of polarization. For this measurement the polarization vector has to be perpendicular to the scattering plane. This can be achieved in a two-step process. Starting from longitudinally polarized electrons, which are produced by illuminating a strained GaAs/GaAsP superlattice photocathode with circularly polarized laser light [13], the electron spin direction will be turned to the transverse orientation (in the horizontal plane) by a Wien filter spin rotator. After that, a pair of solenoids rotates the polarization vector to the vertical orientation. To determine both the magnitude and orientation of the polarization vector, a sophisticated method using Mott and Møller polarimeter - each for itself not capable of measuring directly the vertical polarization component - has been developed [14].

In order to ensure stable, high-quality beam conditions across both orientations of the polarization vector (↑ and ↓) several stabilization systems (beam energy, beam current, and position) were used. The beam stability was ensured by constant measurements with a dedicated monitoring system.

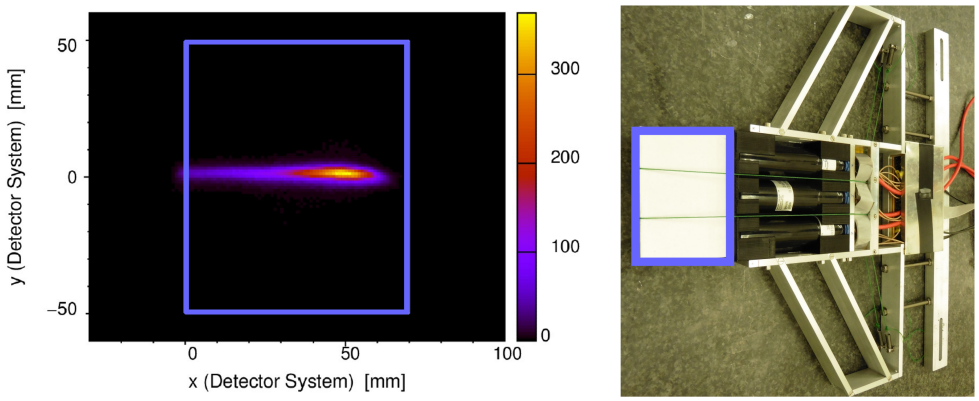

Figure 2: *Left:* Focal plane coordinate system of the high-resolution magnetic spectrometer B. Only coincidence events from the vertical drift chamber and the Cherenkov detector are shown. The blue frame correponds to the size of the fused-silica bar. *Right:* Cherenkov detector which was placed in the focal plane of spectrometer B. The fused-silica bar, marked with the blue frame, is read out with three photomultiplier tubes.

The experiments to systematically study the beam-normal single spin asymmetry were carried out with the spectrometer set-up of the A1 collaboration [15]. Dedicated fused-silica Cherenkov detectors, read out with 25 mm fused-silica-window photomultipliers (see right panel of Fig. 2), were placed in the focal plane of the high-resolution spectrometers A and B. According to the different focal plane geometries of the two spectrometers, the size of the fused-silica bars were chosen to be $(300 \times 70 \times 10)$ mm^3 for spectrometer A and $(100 \times 70 \times 10)$ mm^3 for spectrometer B.
The two Cherenkov detectors were operated in two different modes. In the low beam current mode ($I \approx 20$ nA) the standard A1 readout system [15] was used to read out the Cherenkov detectors in coincidence with the vertical drift chambers of the spectrometers. Based on this information, the elastic line could be placed exactly within the fused-silica bar by changing the magnetic field setting as illustrated in Fig. 2, left panel.
Afterwards the beam current was raised up to 20 µA and all other detector components of the spectrometers were switched off. In this high beam current mode the Cherenkov detectors were read out with the data acquisition electronics from the former A4 experiment [16]. The detector signals from the individual photomultiplier tubes were acquired with analog-to-digital converters, integrating the charge over periods of 20 ms. These integration windows were arranged in a pseudorandom sequence of quadruples with the polarization vector being either ↑↓↓↑ or ↓↑↑↓.
To study the Q^2 dependence of the transverse asymmetry A_n, electrons with a beam energy of 570 MeV were elastically scattered off a 2.27 g/cm^2 carbon target ^{12}C $(\vec{e}, e')^{12}$C. Because of the large energy difference between the ground state and its first excited state ($\Delta E \approx 4.4$ MeV), elastic events could be clearly separated from inelastic ones. To be most sensitive to possible instrumental asymmetries due to helicity correlated changes of the beam parameters, the first measurement was carried out with both spectrometers covering the same Q^2 range. Therefore, spectrometer A was placed at its minimum angle of 23.50°, corresponding to $Q^2 \approx 0.04$ GeV$^2/c^2$. After this first

measurement spectrometer A was moved to a larger angle, covering $Q^2 \approx 0.05\,\mathrm{GeV}^2/c^2$, while spectrometer B was measuring at two smaller angles, corresponding to $Q^2 \approx 0.02\,\mathrm{GeV}^2/c^2$ and $Q^2 \approx 0.03\,\mathrm{GeV}^2/c^2$. Details of the measurement and analysis are given in [17].

To systematically investigate the transverse asymmetry for heavier targets, the same set-up has been used in follow-up experiments. Here, the electrons were elastically scattered off a $1.17\,\mathrm{g/cm}^2$ silicon (^{28}Si) and a $1.11\,\mathrm{g/cm}^2$ zirconium (^{90}Zr) target to study the Z dependence of A_n [18]. The measurements were carried out at $Q^2 \approx 0.04\,\mathrm{GeV}^2/c^2$ to be most sensitive to possible helicity correlated changes of the beam parameters and to allow for a direct comparison with the previous results on carbon [17]. Because of their low melting temperature, both target materials were mounted inside a cooling frame, where a water-ethanol mixture was circulating at a stabilized temperature $T_{\mathrm{circ}} = 0.5°\mathrm{C}$. Moreover, the beam spot was rastered over an area of $4\,\mathrm{mm} \times 4\,\mathrm{mm}$ to better distribute the heat load to avoid any density variations.

4. Results

From the integrated detector signal, which is proportional to the detected number of elastically scattered electrons for each polarization state $N_e^{\uparrow(\downarrow)}$, the raw detector asymmetry

$$A_{\mathrm{raw}} = \frac{N_e^{\uparrow} - N_e^{\downarrow}}{N_e^{\uparrow} + N_e^{\downarrow}} \tag{5}$$

was determined. After accounting for remaining small helicity correlated changes of the beam parameters with correction factors $c_i (i = 1, ..., 6)$, the experimental asymmetry is obtained

$$A_{\mathrm{exp}} = A_{\mathrm{raw}} - c_1 A_I - c_2 \Delta x - c_3 \Delta y - c_4 \Delta x' - c_5 \Delta y' - c_6 \Delta E. \tag{6}$$

The information from the beam monitor system was used to extract the beam current asymmetry A_I, the polarity correlated differences of the horizontal (Δx) and vertical (Δy) position at the target, the corresponding differences in beam angle ($\Delta x'$ and $\Delta y'$) and the beam energy difference ΔE. The results for all three targets ^{12}C, ^{28}Si, and ^{90}Zr are summarized in Tab. 1.

Target	^{12}C					^{28}Si		^{90}Zr	
Spectrometer	B	B	A	A	B	A	B	A	B
Q^2 (GeV^2/c^2)	0.023	0.030	0.049	0.039	0.041	0.038	0.036	0.042	0.042
A_n (ppm)	**-15.984**	**-20.672**	**-28.296**	**-23.877**	**-21.933**	**−23.302**	**−21.807**	**−17.033**	**−16.787**
Systematic error (ppm)	+0.664	+0.551	+0.555	+0.752	+1.621	+0.553	+0.386	+1.390	+1.527
	-0.664	-0.551	-0.555	-0.752	-1.621	−0.531	−0.614	−1.688	−1.622
Statistical error (ppm)	1.061	0.959	1.372	0.967	1.515	1.366	1.389	3.524	5.466

Table 1: Measured beam-normal single spin asymmetries for each spectrometer and kinematics with the corresponding statistical and systematic uncertainty contributions.

The experimentally determined Q^2 dependence of the transverse asymmetry for carbon is shown in Fig. 3 in comparison to the theoretical prediction [11]. Due to limited available Compton form factor data for heavier targets, we assigned 10% (20%) to the uncertainties of the Compton slope parameter B. Although experiment and theory are in good agreement within the given uncertainties,

the experimental results support the hypothesis, that the leading Q^2 behaviour of the asymmetry, given by the ratio of the Compton to charge form factors, cannot be treated independently of the target nucleus.

Because all our measurements related to the Z dependence of the beam-normal single spin asymmetry were performed at the same kinematics, A_n depends only on the mass to charge ratio of the nucleus. Therefore, the measured transverse asymmetry for ^{28}Si can be compared to the same theoretical prediction obtained for ^{12}C. The corresponding theory prediction for ^{90}Zr is given by the blue dash-dotted line in Fig. 3, where the 10% and 20% error bands for the Compton slope parameter are indicated by the blue dashed and dotted lines, respectively.

Due to problems with the vacuum conditions in the scattering chamber, the ^{90}Zr target partially oxidized and formed brittle ZrO_2. For safety and radiation protection reasons the measurement had to be cancelled earlier than intended, which resulted in the large statistical uncertainty.

Within the given uncertainties the experimentally determined values for A_n agree with the theoretical calculations. A dramatic disagreement, as it was obtained for ^{208}Pb [12], has not been observed for ^{90}Zr: though our result is affected by a large statistical uncertainty, its value is not compatible with zero, unlike for the ^{208}Pb measurement.

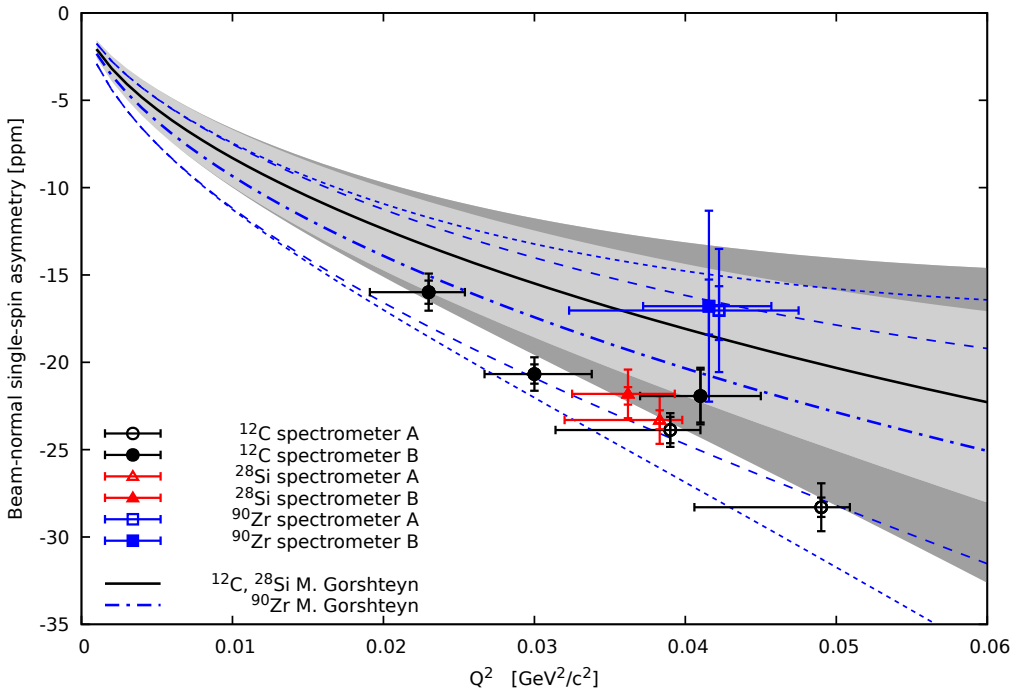

Figure 3: The measured beam-normal single spin asymmetry of ^{12}C (black points), ^{28}Si (red triangles), and ^{90}Zr (blue squares) as a function of Q^2. The open (filled) symbols belong to the data taken with the detector placed in spectometer A (B). The statistical and systematic uncertainties are given by the vertical error bars. For details see Tab. 1. The given horizontal bar corresponds to the full width at half maximum of the Q^2 distribution. The data [17, 18] are compared to the theoretical calculation from Ref. [11]. The assigned uncertainty of 10% (20%) to the Compton slope parameter is given by the light grey (dark grey) bands for ^{12}C and ^{28}Si and by the blue dashed (blue dotted) lines for ^{90}Zr.

5. Outlook

The systematic study of the Q^2 and Z dependence of the beam-normal single spin asymmetry shows, that more comprehensive studies of the Compton slope parameter are essential to advance our current understanding of the process. In order to reduce the uncertainty of the Compton slope parameter for intermediate mass nuclei, an independent determination of this quantity for the kinematics used in the transverse asymmetry measurements seems to be mandatory. Feasibility studies are currently undertaken to investigate the use of the CATS NaI detector [19] with a tagged photon beam at A2@MAMI to measure Compton scattering from ^{12}C above the $\Delta(1232)$ resonance at forward angles. This will enable us to obtain the Compton form factor at different Q^2 values and extract the Compton slope parameter B with improved precision.
This information can be used to further refine the theoretical calculation for the transverse asymmetry and address the disagreement between experimental and theoretical results for ^{208}Pb. Although more data for the beam-normal single spin asymmetry for ^{12}C, ^{27}Al [20], as well as for ^{12}C, ^{40,48}Ca, and ^{208}Pb [21] are available nowadays and while no significant disagreement could be observed for the lighter nuclei, the observed discrepancy between experiment and theory for ^{208}Pb still persists. We will therefore expand our systematic study of the transverse asymmetry to ^{208}Pb. Measuring at the same four-momentum transfer $Q^2 \approx 0.04\,\mathrm{GeV}^2/c^2$, the rates will be significantly lower compared to carbon, because the cross section has a minimum close to this Q^2 value. Thus, the current readout electronics system needs to be modified. The data acquisition electronics from the former A4 experiment we used so far was made for the read out of very high rate luminosity monitors, where the output was nearly a constant current which was read out by analog integrators. A concept which is no longer applicable for much lower count rates as expected for ^{208}Pb. Therefore, we built a new readout electronics system by using fast discriminators, where the individual photomultiplier tube pulses are counted, while the measured beam parameters, which are needed to correct the data for beam fluctuations, are digitized by voltage-to-frequency converters. The new electronics system was successfully tested in various test beams with carbon and natural lead targets. The experiment on isotopically enriched ^{208}Pb at $Q^2 \approx 0.04\,\mathrm{GeV}^2/c^2$ is foreseen for summer 2024. This data will provide important information to the standing discrepancy between experiment and theory and will further enhance our understanding of TPE processes.

6. Acknowledgments

The authors would like to thank the MAMI operators, the accelerator group, the A1 and A4/P2 collaborations, and all the workshop staff members for the outstanding support.
This work was supported by the PRISMA+ (Precision Physics, Fundamental Interactions and Structure of Matter) Cluster of Excellence, the Deutsche Forschungsgemeinschaft through the Collaborative Research Center 1044, the Deutsche Forschungsgemeinschaft through the individual grant No. 454637981, and the Federal State of Rhineland-Palatinate.

References

[1] D. Androić et al., *Precision measurement of the weak charge of the proton*, Nature **557** (2018) 207.

[2] F. E. Maas et al., *Measurement of strange quark contributions to the nucleon's form-factors at $Q^2 = 0.230$ (GeV/c)^2*, Phys. Rev. Lett. **93** (2004) 022002.

[3] D. S. Armstrong et al., *Strange quark contributions to parity-violating asymmetries in the forward G0 electron-proton scattering experiment*, Phys. Rev. Lett. **95** (2005) 092001.

[4] K. A. Aniol et al., *Constraints on the nucleon strange form-factors at $Q^2 \sim 0.1$ GeV^2*, Phys. Lett. B **635** (2006) 275.

[5] D. Adhikari et al., *Accurate Determination of the Neutron Skin Thickness of ^{208}Pb through Parity-Violation in Electron Scattering*, Phys. Rev. Lett **126** (2021) 172502.

[6] D. Adhikari et al., *Precision Determination of the Neutral Weak Form Factor of Ca48*, Phys. Rev. Lett. **129** (2022) 042501.

[7] J. Benesch et al., *The MOLLER Experiment: An Ultra-Precise Measurement of the Weak Mixing Angle Using Møller Scattering*, arXiv:1411.4088, 2014.

[8] J. P. Chen et al., *A White Paper on SoLID (Solenoidal Large Intensity Device)*, arXiv:1409.7741, 2014.

[9] D. Becker et al., *The P2 experiment*, Eur. Phys. J. A **54** (2018) 208.

[10] A. De Rujula et al., *Elastic scattering of electrons from polarized protons and inelastic electron scattering experiments*, Nucl. Phys. B **35** (1971) 365.

[11] M. Gorchtein and C. J. Horowitz, *Analyzing power in elastic scattering of the electrons off a spin-0 target*, Phys. Rev. C **77** (2008) 044606.

[12] S. Abrahamyan et al., *New Measurements of the Transverse Beam Asymmetry for Elastic Electron Scattering from Selected Nuclei*, Phys. Rev. Lett. **109** (2012) 192501.

[13] K. Aulenbacher et al., *The MAMI source of polarized electrons*, Nucl. Instrum. Meth. A **391** (1997) 498.

[14] B. S. Schlimme et al., *Vertical Beam Polarization at MAMI*, Nucl. Instrum. Meth. A **850** (2017) 54.

[15] K. I. Blomqvist et al., *The three-spectrometer facility at the Mainz microtron MAMI*, Nucl. Instrum. Meth. A **403** (1998) 263.

[16] F. E. Maas et al., *Parity violating electron scattering at the MAMI facility in Mainz: The Strangeness contribution to the form-factors of the nucleon*, Eur. Phys. J. A **17** (2003) 339.

[17] A. Esser et al., *First Measurement of the Q^2 Dependence of the Beam-Normal Single Spin Asymmetry for Elastic Scattering off Carbon*, Phys. Rev. Lett. **121** (2018) 022503.

[18] A. Esser et al., *Beam-normal single spin asymmetry in elastic electron scattering off ^{28}Si and ^{90}Zr*, Phys. Lett. B **808** (2020) 135664.

[19] F. Wissmann et al., *Elastic and inelastic photon scattering from C-12*, Phys. Lett. B **335** (1994) 119.

[20] D. Androić et al., *Measurement of the Beam-Normal Single-Spin Asymmetry for Elastic Electron Scattering from ^{12}C and ^{27}Al*, Phys. Rev. C **104** (2021) 014606.

[21] D. Adhikari et al., *New Measurements of the Beam-Normal Single Spin Asymmetry in Elastic Electron Scattering over a Range of Spin-0 Nuclei*, Phys. Rev. Lett. **128** (2022) 142501.